



Cite this: *Food Funct.*, 2021, **12**, 6363

Lactobacillus plantarum HAC01 ameliorates type 2 diabetes in high-fat diet and streptozotocin-induced diabetic mice in association with modulating the gut microbiota†

Young-Sil Lee, Daeyoung Lee, Gun-Seok Park, Seung-Hyun Ko, Juyi Park,
You-Kyung Lee and Jihee Kang  *

Type 2 diabetes mellitus (T2DM) is a serious metabolic disorder that occurs worldwide; however, this condition can be managed with probiotics. We assessed the potential therapeutic effects of *Lactobacillus plantarum* HAC01 on hyperglycemia and T2DM and determined their potential mechanisms using mice with high-fat diet (HFD) and streptozotocin (STZ)-induced diabetes. The diabetic model was established with an HFD and 50 mg kg⁻¹ STZ. *L. plantarum* HAC01 was then administered for 10 weeks. Body weight, food and water intake, biochemical parameters, and homeostasis model assessment for insulin resistance (HOMA-IR) were measured. Oral glucose tolerance test and histological analysis were performed, and the glucose metabolism-related gene expression and signaling pathways in the liver were determined. Fecal microbiota and serum short-chain fatty acids (SCFAs) were also analyzed. *L. plantarum* HAC01 significantly lowered blood glucose and HbA1c levels and improved glucose tolerance and HOMA-IR. Additionally, it increased the insulin-positive β -cell area in islets and decreased the mRNA expression levels of phosphoenolpyruvate carboxykinase and glucose 6-phosphatase, which are associated with gluconeogenesis. *L. plantarum* HAC01 also increased the phosphorylation of AMPK and Akt, which are involved in glucose metabolism in the liver. Notably, *L. plantarum* HAC01 increased the Akkermansiaceae family and increased SCFAs in serum. *L. plantarum* HAC01 could alleviate hyperglycemia and T2DM by regulating glucose metabolism in the liver, protecting the islet β -cell mass, and restoring the gut microbiota and SCFAs. *L. plantarum* HAC01 may thus be an effective therapeutic agent for T2DM.

Received 5th March 2021,

Accepted 14th May 2021

DOI: 10.1039/d1fo00698c

rsc.li/food-function

1. Introduction

Type 2 diabetes mellitus (T2DM) has become a public health burden globally. According to a report by the International Diabetes Federation, the number of patients with diabetes will increase to 415 million by 2040.¹ T2DM is a chronic metabolic disorder that is characterized by hyperglycemia, which is mainly caused by impaired insulin secretion and insulin resistance.^{2,3} Insulin regulates glucose metabolism in target tissues, such as the liver, muscle, and adipose tissues. In particular, the liver plays an important role in glucose homeostasis by balancing gluconeogenesis and glycogen synthesis. Insulin resistance in the liver and impaired ability to secrete insulin contributes to hyperglycemia and T2DM.⁴ However, as research on gut microbiota progresses, compelling evidence

supports the crucial role of gut microbiota in the progression and development of T2DM.⁵ The gut microbiota may affect intestinal permeability as well as metabolic and signaling pathways, including systemic inflammation, gut hormone release, and energy and glucose metabolism. Thus, changes in the composition and structure of the gut microbiota, termed "dysbiosis", and the imbalance of gut microbiota may contribute to the pathogenesis of T2DM.⁶⁻⁸ Regarding to these, short-chain fatty acids (SCFAs) have been identified as a link between gut microbiota and T2DM. SCFAs from the gut are rapidly transferred to blood system and regulate glucose and lipid metabolism with multiple mechanisms through activation of SCFA receptors and inhibition of histone deacetylase (HDACs).^{5,9,10} SCFAs affect gut barrier function and the gut immune system, leading to prevent low-grade chronic inflammation in adipose tissue and onset of diabetes.^{9,10} In addition, SCFAs are natural inhibitors of HDACs that modulate the expression of critical genes involved in pathogenesis of diabetes. Among SCFAs, butyrate is reported to reduce the gluconeogenesis and glycogenolysis by inhibiting HDACs.^{5,9,10}

AtoGen Co., Ltd, Daejeon, 34015, Korea. E-mail: jhkang@atogen.co.kr;

Tel: +82-42-931-8254; Fax: +82-42-931-8257

† Electronic supplementary information (ESI) available. See DOI: [10.1039/d1fo00698c](https://doi.org/10.1039/d1fo00698c)



Besides SCFAs increase the β -cell mass and function through SCFA receptor-mediated signaling or by indirectly increasing GLP-1 secretion from enteroendocrine L-cell and they promote the glucose-mediated insulin secretion.^{9,10} Therefore, gut microbiota could thus serve as a new target for T2DM management.^{11,12}

Being composed of microorganisms that form an important part of gut microbiota, probiotics have been proven to have beneficial effects on human health; this is because they can alter the host's gut microbiota.¹³ Among them, *Lactobacillus* is known to prevent or treat T2DM. Previously, *Lactobacillus acidophilus* and *L. acidophilus* La5 and *Bifidobacterium animalis* subsp. *lactis* Bb12 were demonstrated to improve insulin sensitivity in clinical studies.^{14,15} In addition, *Lactobacillus casei* CCFM419, *Lactobacillus reuteri* GMNL-263, *Lactobacillus rhamnosus* GG (LGG), and *Lactobacillus paracasei* NL41 were found to alleviate insulin resistance and hyperglycemia in diabetic rats.¹⁶⁻¹⁹ Although different studies have demonstrated the anti-diabetic effect of probiotics, their molecular mechanisms have not been fully investigated. Moreover, probiotics exert species-specific and strain-specific effects and employ different mechanisms.^{12,19} Therefore, discovering more probiotic strains with functional features specific for T2DM is warranted.

Lactobacillus plantarum HAC01 is a novel probiotic isolated from Korean white kimchi (baek kimchi). The isolation and identification of *L. plantarum* HAC01 has been reported,²⁰ and proved the safety as probiotics properties and exhibited functional effects such as anti-obesity effect and anti-hyperlipidemia effect.^{20,21} In this study, we sought to investigate the beneficial effects of *L. plantarum* HAC01 on T2DM and its underlying mechanism for ameliorating T2DM in high-fat diet (HFD) + streptozotocin (STZ)-induced diabetic mice.

2. Materials and methods

2.1. Preparation of *Lactobacillus plantarum* HAC01

Lactobacillus plantarum HAC01 has been deposited in the Korean Collection for Type Culture (KCTC; WDCM597) under the number, KCTC 12647BP.²⁰ The strain was incubated in de Man Rogosa Sharp broth (Difco Laboratories Inc., Franklin Lakes, NJ, USA) at 37 °C for 16 h. Thereafter, the cells were retrieved via centrifugation (3000g, 10 min, 4 °C) and washed three times with PBS (pH 7.4). The cell pellets were resuspended to 1×10^9 and 4×10^9 CFU per 200 μ l in PBS and prepared daily throughout the experimental period.

2.2. Animal experiments

C67BL/6J (five weeks old, male) were purchased from Central Lab Animal Inc. (Seoul, Korea). Mice were housed under environmental conditions (temperature: 22 °C \pm 2 °C, humidity: 55% \pm 5%, and 12 h light/dark cycle), with free access to food and water throughout the experiments. The study protocol was approved by the Atogen Animal Care and Use Committee (ATG-IACUC-RDSB-200713), and animal studies

were carried out in accordance with the guidelines established by the committee. After 1 week of acclimatization, mice were divided into the following five groups ($n = 10$): (1) NFD group (4.5 kcal% fat), (2) HFD (60 kcal% Fat, D12492 (Table S1†), Research diet, New Brunswick, NJ, USA) + Streptozotocin (Sigma-Aldrich)_control group (HFD + STZ_Con), (3) HFD + STZ_1 \times 10^9 CFU viable cell of HAC01 (HFD + STZ_1 \times 10^9 CFU HAC01), (4) HFD + STZ_4 \times 10^9 CFU viable cell of HAC01 (HFD + STZ_4 \times 10^9 CFU HAC01), and (5) HFD + STZ_300 mg kg⁻¹ metformin (HFD + STZ_Met300). Every group was administered an HFD for 1 to 10 weeks, except the NFD group. In week 5, mice administered an HFD were injected intraperitoneally with 50 mg kg⁻¹ of STZ freshly dissolved in 0.1 M citrate buffer (pH 4.5) for five consecutive days to induce T2DM, while the NC group received an intraperitoneal injection of an equivalent volume of 0.1 M citrate buffer. *L. plantarum* HAC01 at doses of 1×10^9 and 4×10^9 CFU day⁻¹ and metformin at a dose of 300 mg kg⁻¹ were orally administered for 10 weeks. The NFD and HFD + STZ_con groups were administered PBS via oral gavage. Body weight and the food and water intake rates of animals were recorded twice per week.

2.3. OGTT

OGTT was performed 9 weeks after *L. plantarum* HAC01 treatment. Mice were fasted for 12 h and blood glucose levels (0 min) were measured. Thereafter, mice were orally administered glucose (1 g per kg body weight), and their blood glucose levels were measured at 30, 60, and 120 min using a glucometer (G-doctor, allmedicus, Anyang, Gyeonggi-do, Korea). The area under the curve for blood glucose (AUC_{glu}) over 2 h was calculated.

2.4. Blood, tissues (liver and pancreas), and feces collection

At the end of the experiment, mice were anesthetized and killed after a 12 h fasting. After blood samples were collected, they were centrifuged to obtain serum. The separated serum samples were then stored at -80 °C until analysis. Liver samples were immediately excised, rinsed, weighed, frozen in liquid nitrogen, and stored at -80 °C until analysis. Pancreas samples were fixed in formalin until histological analysis. Feces were collected in sterile tubes and stored at -80 °C until analysis.

2.5. Serum biochemical parameter analysis

Fasting glucose levels were analyzed using a glucometer. Serum HbA1c levels were determined enzymatically using commercial assay kits (BioVision, Milpitas, CA, USA). Serum insulin levels were determined using an ELISA kit (mouse ultrasensitive insulin ELISA, ALPCO, Salem, NH). Homeostatic model assessment of insulin resistance (HOMA-IR) was calculated using the following equation: HOMA = fasting glucose level \times fasting insulin level/405.

2.6. RNA isolation and gene expression analyses

Total RNA was isolated from liver samples using a RNeasy mini kit (Qiagen, Valencia, CA). Thereafter, total RNA was

Table 1 PCR primers sequences genes

	Primers sequences (5' → 3')
Phosphoenolpyruvate carboxykinase (<i>PEPCK</i>)	Forward: CTG CAT AAC GGT CTG GAC TTC Reverse: CAG CAA CTG CCC GTA CTC C
Glucose 6-phosphatase (<i>G6Pase</i>)	Forward: CGA CTC GCT ATC TCC AAG TGA Reverse: GTT GAA CCA GTC TCC GAC CA
β-Actin	Forward: TCT ACG AGG GCT ATG CTC TCC Reverse: GGA TGC CAC AGG ATT CCA TAC

reverse-transcribed to cDNA with oligo primers in a reverse transcription system (AccuPower RT PreMix, Bioneer, Daejeon, Korea), according to the manufacturer's protocol. Real-time PCR was performed using 100 ng of cDNA template, primers, and a PowerUp SYBR green Master Mix (Applied Biosystems, Foster City, CA, USA) on an ABI Prism 7500 Fast Real-Time PCR system (Applied Biosystems, USA), according to the manufacturer's protocol. The primer sequences were given in Table 1. All samples were normalized to the corresponding expression of β-actin. The expression level of the target genes relative to their expression level in the HFD + STZ_Con group was calculated using the comparative Ct method.

2.7. Protein extraction and western blotting

Liver protein was extracted with RIPA lysis buffer (Millipore, Billerica MA, USA) and protein concentration was determined using a Pierce BCA protein assay kit (Thermo Fisher Scientific, IL, USA) using bovine serum albumin as a standard. Proteins were transferred onto PVDF membranes (Bio-Rad, USA) following separation *via* SDS-PAGE. The membranes were blocked with blocking solution (Thermo Fisher Scientific, IL, USA), and incubated overnight at 4 °C with specific primary antibodies against *p*-AMPK, AMPK, *p*-Akt, Akt, and GAPDH (Cell Signaling Technology, Beverley, MA, USA) and horseradish peroxidase-conjugated secondary antibodies (Santa Cruz Biotechnology, Santa Cruz, CA, USA). The immunocomplexes were developed by chemiluminescence and images were analyzed using Image Lab software (Bio-Rad, USA). The relative protein expression levels were calculated as a ratio to HFD + STZ_Con expression.

2.8. Immunocytochemistry

Tissues were fixed (10% formalin solution in 0.1 M PBS), paraffin-embedded, and cut into 4-μm sections on a microtome. Prior to incubation with the primary antibody, the tissue sections were permeabilized in 0.1% Triton X-100 in PBS and blocked in 5% normal goat serum and 0.1% Triton X-100 in PBS. Islets were stained with insulin Alexa Fluor® 488 (eBioscience, San Diego, CA, USA) and DAPI nuclear stain (Sigma-Aldrich, St Louis, MO, USA). Images were acquired with an Axiovert 40 CFL confocal microscope (Carl Zeiss, Oberkochen, Germany).

2.9. Fecal microbiota analysis

Genomic DNA extraction from fecal samples was performed using the QIAamp PowerFecal Pro DNA Kit (Qiagen, Germany).

The quantity and quality of extracted DNA were measured using a Qubit 3.0 Fluorometer (Thermo Fisher Scientific, USA) and agarose gel electrophoresis, respectively. The V4 hypervariable regions of the bacterial 16S rRNA were amplified with unique 8 bp barcodes and sequenced on the Illumina MiSeq PE300 platform using the standard protocol.²² The raw sequence data were submitted to the NCBI SRA database (NCBI BioProject PRJNA693106, raw data accession number). Raw reads were analyzed using the QIIME pipeline.²³ Sequences were quality filtered and clustered into operational taxonomic units at 97% sequence identity, according to the SILVA 132 database.²⁴ Operational taxonomy units were identified at the phylum to genus levels. The weighted UniFrac distances were previously obtained and used for principal coordinate analysis (PCoA).²⁵

2.10. Analysis of serum SCFAs

2.10.1. Chemicals. Acetic acid (\geq 99.8% purity), butyric acid (\geq 99.5% purity), and propionic acid (\geq 99.5% purity) were of analytical grade and were purchased from Sigma-Aldrich (St Louis, MO, USA). Formic acid (\geq 99.5% purity), ammonium formate (\geq 99.995% purity), acetonitrile (ACN), methanol (MeOH), and water were purchased from Sigma-Aldrich. All solvents were of high-performance liquid chromatography grade.

2.10.2. Sample preparation. Sample preparation was achieved *via* protein removal. Briefly, 100 μ L of serum was mixed with 500 μ L of ice-cold MeOH and 1% formic acid. After the solution was thoroughly mixed *via* a 20 min vortex, it was left for 2 h (4 °C) to enable solidification of the precipitate. After centrifugation at 14 000 rpm for 30 min at 4 °C, the supernatant was filtered using a PVDF 0.22 μ m pore size syringe filter (Millipore, Billerica, MA). The filtered sample was then injected into the liquid chromatography-tandem mass spectrometry (LC-MS/MS) system.

2.10.3. LC-MS/MS instrumentation and analytical conditions. LC-MS/MS analyses were carried out using an Exion LC system connected to a QTRAP 4500 mass spectrometer (AB SCIEX, Framingham, MA, USA). Separation was achieved with an Intrada Organic Acid column (150 × 2 mm, 3 μ m particle size, Imtakt Kyoto, JPN) at a flow rate of 0.2 mL min⁻¹ and column temperature of 40 °C. An injection volume of 5 μ L was used for the autosampler injection. In positive ion mode, a gradient mobile phase consisting of (A) acetonitrile : water : formic acid 10 : 90 : 0.1 [v/v] solution and (B) acetonitrile:100 mM ammonium formate 10 : 90 solution was employed. For gradient elution, (A)/(B) ratios were used from 100/0 hold at 1 min, 0/100 between 1 and 7 min, a 3 min hold at 100% (B), and a final return to 100% (A) within 0.1 min; total run time was 15 min. The analysis was carried out using an electrospray ionization source in negative mode. The operating conditions were: ion spray voltage, 4500 V; curtain gas (CUR), 25 psi; collision gas (CAD), medium; ion source gas 1 (GS1) and ion source gas 2 (GS2), 50 and 50 psi; turbo spray temperature (TEM), 450 °C; entrance potential (EP), 10 V; and collision cell exit potential (CXP), 5 V. Nitrogen was employed



in all cases. Analytes were quantified by multiple reaction monitoring using the following precursor to product ion transitions and parameters: acetic acid, m/z 105.0 \rightarrow 44.9 with declustering potential (DP) 5 V and collision energy (CE) 18 eV; butyric acid, m/z 133.0 \rightarrow 44.9 with DP 5 V and CE 18 eV; propionic acid, m/z 119.0 \rightarrow 45.1 with DP 5 V and CE 16 eV. SCIEX OS 2.0.0 software was used for data acquisition and processing while Analyst 3.3 software was used for data analysis.

2.11. Statistical analysis

Data are presented as mean \pm SEM. Differences between groups were assessed using one-way ANOVA followed by Dunnett's multiple comparison tests with Prism 8.0 software (GraphPad Software Inc., San Diego, CA, USA). In the cases of diversity indexes and microbial taxa were analyzed by non-parametric Kruskal-Wallis test. A p value <0.05 was considered to indicate statistical significance.

3. Results

3.1. Effect of *L. plantarum* HAC01 on body weight, food intake, and water intake

During the first phase of HFD feeding for 4 weeks, there was an increase in body weight in the HFD + STZ_Con and HFD + STZ_HAC01 groups; however, no significant difference was found between the groups. In contrast, treatment with Met300 significantly prevented any increase in body weight. Following STZ injection, body weight was reduced in all HFD-fed groups at 1 week, with no significant difference found among the groups (Fig. 1A). Food and water intake rates in the HFD + STZ_Con group were higher than those in the normal fat diet (NFD) group. However, no significant difference was observed between the HFD + STZ_Con group and *L. plantarum* HAC01 groups, despite the decreased water intake rate in the Met300 group (Fig. 2B and C).

3.2. Effect of *L. plantarum* HAC01 on fasting glucose, HbA1c, insulin levels and HOMR-IR

Fasting glucose and HbA1c levels in the HFD + STZ_Con group were significantly higher than those in the NFD group; however, these levels were lowered in the HFD + STZ-induced diabetic mice administered 4×10^9 CFU of *L. plantarum* HAC01 and Met300 (Fig. 2A and B). Additionally, treatment with 4×10^9 CFU of *L. plantarum* HAC01 and Met300 remarkably reduced HOMA-IR compared to HFD + STZ_Con treatment, despite no significant difference in insulin levels (Fig. 2C and D). These results suggest that *L. plantarum* HAC01 exhibits an anti-hyperglycemic effect in the HFD + STZ-induced diabetic model.

3.3. Effects of *L. plantarum* HAC01 on OGTT

To determine the effects of *L. plantarum* HAC01 on glucose tolerance, OGTT was performed after 9 weeks of treatment. As shown in Fig. 3, glucose tolerance was impaired in the HFD + STZ_Con group (*i.e.*, the glucose levels were higher at all time points after glucose administration). In addition, AUC_{glucose} during OGTT was higher than that in the NFD group. However, treatment with 4×10^9 of *L. plantarum* HAC01 and Met300 inhibited the increase in glucose levels at 30 and 60 min during OGTT. Similarly, treatment with 4×10^9 CFU of *L. plantarum* HAC01 and Met300 significantly reduced the AUC compared to that found in the HFD + STZ_Con group. These results suggest that *L. plantarum* HAC01 improves glucose intolerance in the HFD + STZ-induced diabetic model.

3.4. Effects of *L. plantarum* HAC01 on the expression of genes related to glucose metabolism in the liver

To determine the effect of *L. plantarum* HAC01 on endogenous hepatic glucose production, the expression of genes and proteins associated with glucose metabolism in the liver were investigated. Relative *p*-AMPK levels and *p*-Akt levels were increased in the 4×10^9 CFU of *L. plantarum* HAC01 and Met300 groups compared to those in the HFD + STZ_Con

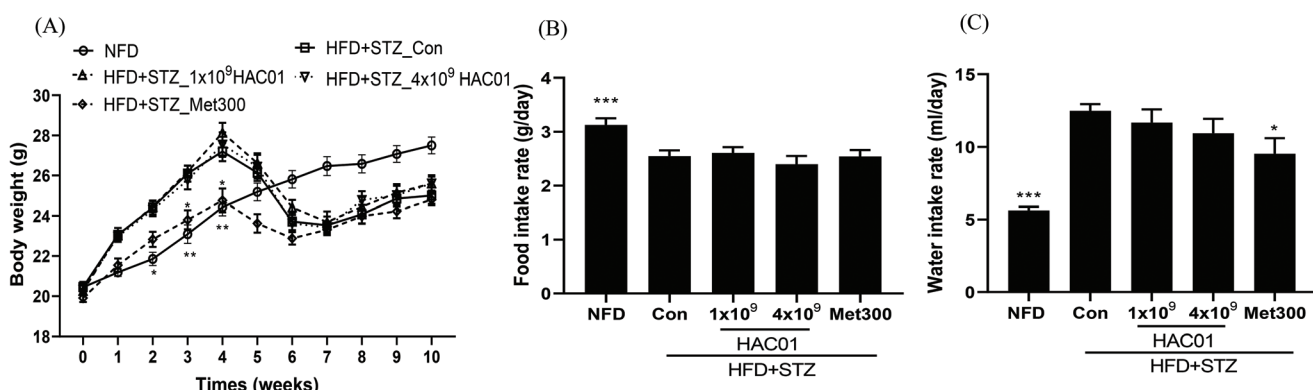


Fig. 1 Effect of *L. plantarum* HAC01 on body weight and the intake rates of food and water in HFD + STZ-induced diabetic mice. (A) Body weight, (B) Food intake rate, and (C) Water intake rate. NFD: Normal fat diet; HFD + STZ_Con: High-fat diet + streptozotocin (STZ); HFD + STZ_1 \times 10⁹–4 \times 10⁹ CFU day⁻¹ *L. plantarum* HAC01; Met300: Metformin 300 mg kg⁻¹. Data are expressed as mean \pm SEM ($n = 10$). * $p < 0.05$, ** $p < 0.01$ and *** $p < 0.005$ vs. the HFD + STZ_Con group.



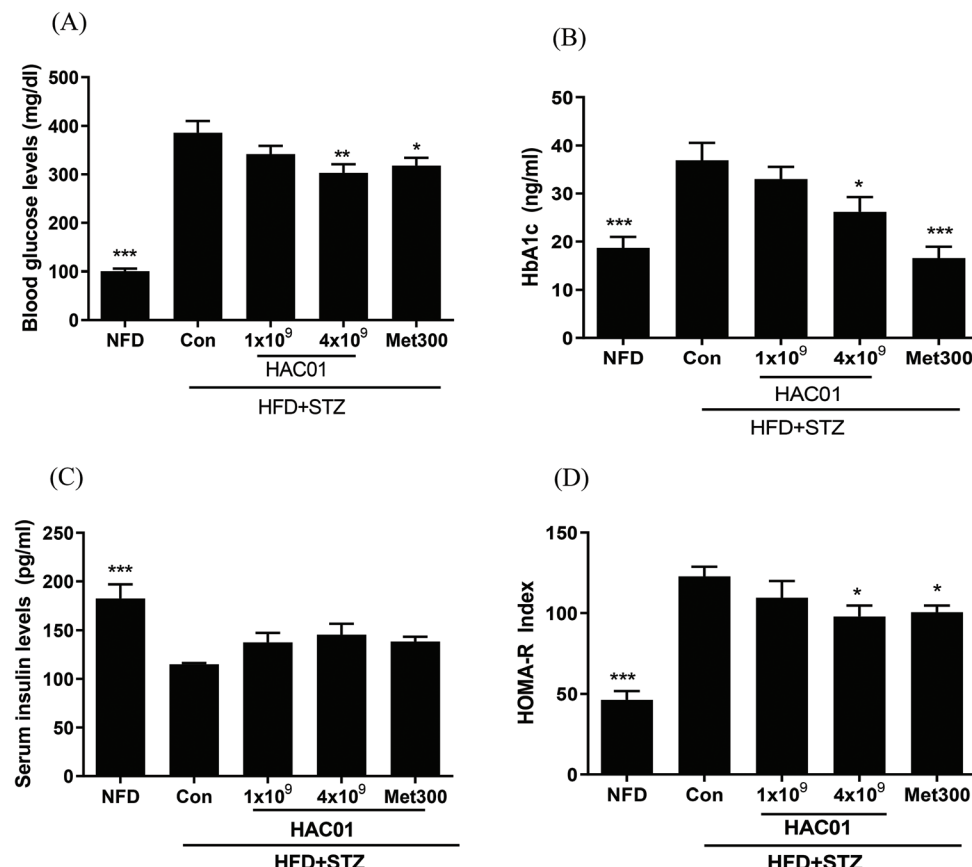


Fig. 2 Effect of *L. plantarum* HAC01 on the biochemical parameters in HFD + STZ-induced diabetic mice. (A) Fasting glucose levels, (B) HbA1c levels, (C) Insulin levels, and (D) HOMA-IR. NFD: Normal fat diet; HFD + STZ_Con: High-fat diet + streptozotocin (STZ); HFD + STZ_1 \times 10⁹–4 \times 10⁹ HAC01: HFD + STZ + 1 \times 10⁹–4 \times 10⁹ CFU day⁻¹ *L. plantarum* HAC01; Met300: Metformin 300 mg kg⁻¹. Data are expressed as mean \pm SEM ($n = 10$). *p < 0.05, **p < 0.01 and ***p < 0.005 vs. the HFD + STZ_Con group.

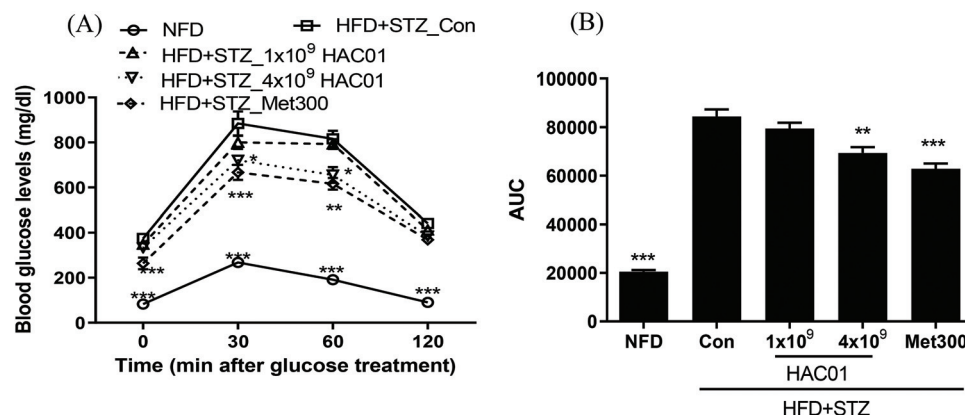


Fig. 3 Effect of *L. plantarum* HAC01 on OGTT in HFD + STZ-induced diabetic mice. (A) OGTT and (B) AUC during OGTT. NFD: Normal fat diet; HFD + STZ_Con: High-fat diet + streptozotocin (STZ); HFD + STZ_1 \times 10⁹–4 \times 10⁹ HAC01: HFD + STZ + 1 \times 10⁹–4 \times 10⁹ CFU day⁻¹ *L. plantarum* HAC01; Met300: Metformin 300 mg kg⁻¹. Data are expressed as mean \pm SEM ($n = 10$). *p < 0.05, **p < 0.01 and ***p < 0.005 vs. the HFD + STZ_Con group.

group (Fig. 4A and B). Moreover, the mRNA expression levels of gluconeogenesis-related genes, such as *PEPCK* and *G6Pase*, were markedly suppressed in the HFD + STZ_HAC01 (1 \times 10⁹ and 4 \times 10⁹ CFU) and Met300 groups compared to those in the

HFD + STZ_Con group (Fig. 4C and D). Such findings imply that *L. plantarum* HAC01 exerts anti-hyperglycemic effects by reducing gluconeogenesis in the HFD + STZ-induced diabetic model.

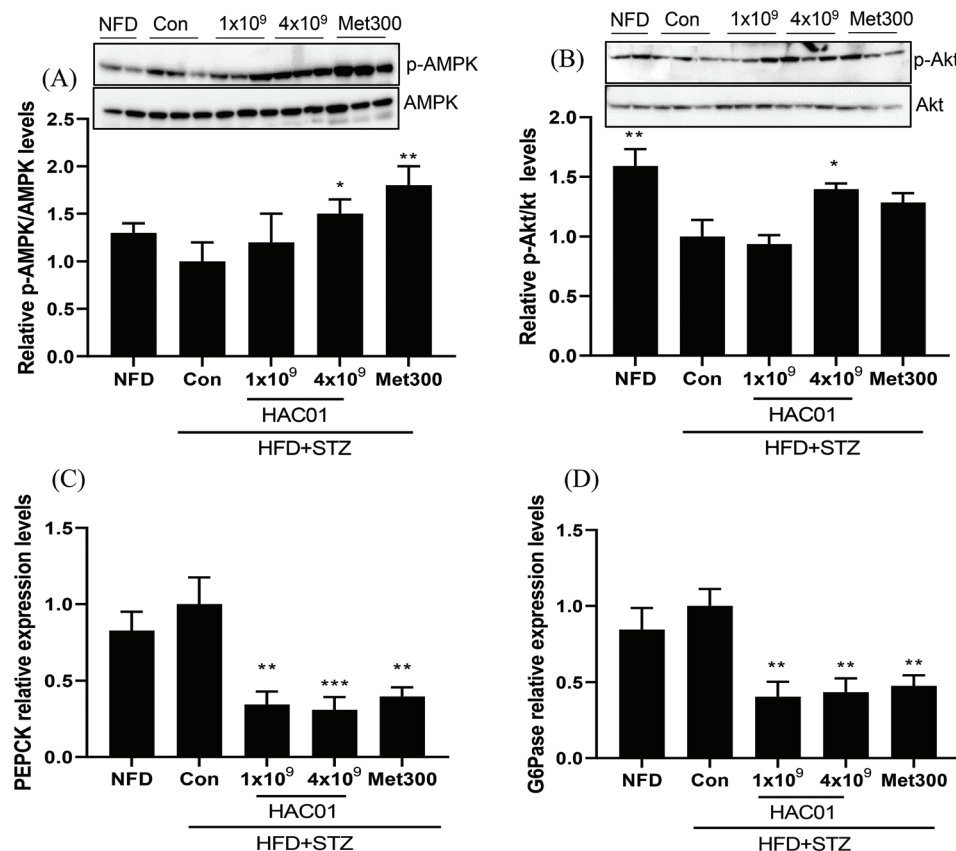


Fig. 4 Effect of *L. plantarum* HAC01 on glucose metabolism in the liver of HFD + STZ-induced diabetic mice. (A) Relative p-AMPK/AMPK expression levels, (B) Relative p-Akt/Akt expression levels, (C) PEPCK mRNA expression levels, and (D) G6Pase mRNA expression levels. NFD: Normal fat diet; HFD + STZ_Con: High-fat diet + streptozotocin (STZ); HFD + STZ_1 \times 10⁹–4 \times 10⁹ HAC01: HFD + STZ + 1 \times 10⁹–4 \times 10⁹ CFU day⁻¹ *L. plantarum* HAC01; Met300: Metformin 300 mg kg⁻¹. *p < 0.05, **p < 0.01 and ***p < 0.005 vs. the HFD + STZ_Con group.

3.5. Immunofluorescence analysis of islet β cells in the pancreas

Histological analysis of the pancreas revealed differences in the pattern and number of islets following treatment with 4 \times 10⁹ CFU of *L. plantarum* HAC01 compared to HFD + STZ_con. The addition of 4 \times 10⁹ CFU of *L. plantarum* HAC01 improved histological abnormalities, including the decreased number of islets and irregular islet morphology and atrophy (data not shown). To further assess the effect of *L. plantarum* HAC01 on islet morphology, insulin immunofluorescence staining was performed. As shown in Fig. 5, relative insulin-positive cells were reduced and irregularly-shaped morphology was observed in the HFD + STZ_con group; however, these cells were significantly increased in the 4 \times 10⁹ CFU of *L. plantarum* HAC01 group, aligning with the results of H&E staining.

3.6. Modulation of gut microbiota by *L. plantarum* HAC01

To determine the effects of *L. plantarum* HAC01 on the gut microbiota, the bacterial community in fecal samples obtained from each experimental group was analyzed. At the phylum

level, the population of Verrucomicrobia significantly increased in the 4 \times 10⁹ *L. plantarum* HAC01 and Met300 treatment groups compared to those in the other groups (Fig. S1†). The family, Akkermansiaceae (phylum Verrucomicrobia), displayed the same pattern of population shifts in the family-level community analysis as that observed in the phylum level analysis (Fig. 6A and B). The relative abundance of the family, Dusulfovibrionaceae (phylum Proteobacteria), showed the tendency to decrease in the 4 \times 10⁹ CFU of *L. plantarum* HAC01 and Met300 groups (Fig. 6C). The linear discriminant analysis (LDA) effect size (LEfSe) analysis results shows more abundant taxa in 4 \times 10⁹ HAC01-treated group compared to the control group. The family of Propionibacteriaceae, Clostridiaceae1, uncultured rumenbacterium and Akkermansiaceae were enriched in 4 \times 10⁹ HAC01-treated group (Fig. S2†). Compared to other HFD + STZ-induced diabetic groups, Met300 treated group shows decreased value of chao1 and Simpson's index (Fig. S3†). Beta-diversity was assessed via principal coordinate analysis (PCoA) to compare the composition of microbiota using UniFrac distance. Weighted UniFrac takes into account the relative abundance of species/taxa shared between samples. The microbiota from the NFD group were separated



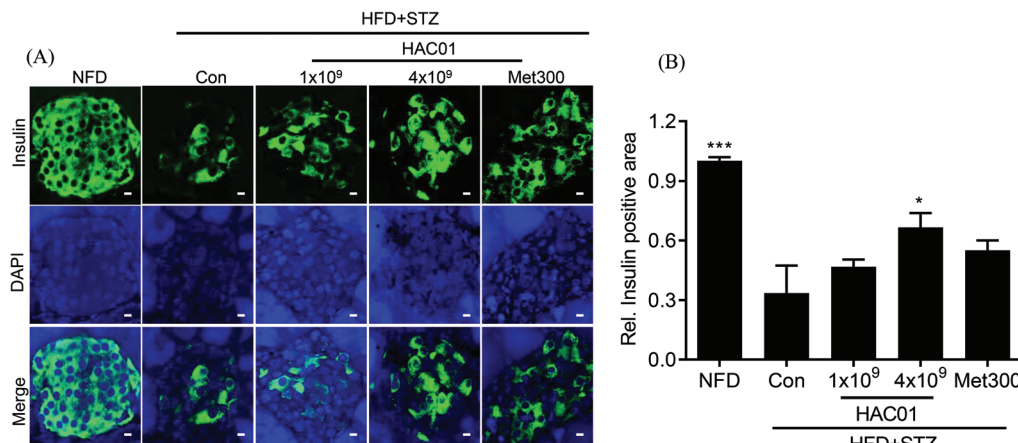


Fig. 5 Effect of *L. plantarum* HAC01 on the destruction of the pancreatic islet. (A) Representative images of pancreatic tissue sections stained for immunofluorescence detection of insulin (insulin staining in green, nuclei staining in blue). All images were captured at 400x magnification. Bars = 20 μ m. (B) Relative insulin-positive areas were quantified using the iSolution DT 36 software. NFD: Normal fat diet; HFD + STZ_Con: High-fat diet + streptozotocin (STZ); HFD + STZ_1 \times 10⁹–4 \times 10⁹ HAC01: HFD + STZ + 1 \times 10⁹–4 \times 10⁹ CFU day⁻¹ *L. plantarum* HAC01; Met300: Metformin 300 mg kg⁻¹. Data are expressed as mean \pm SEM (n = 5). * p < 0.05, and ** p < 0.01 vs. the HFD + STZ_Con group.

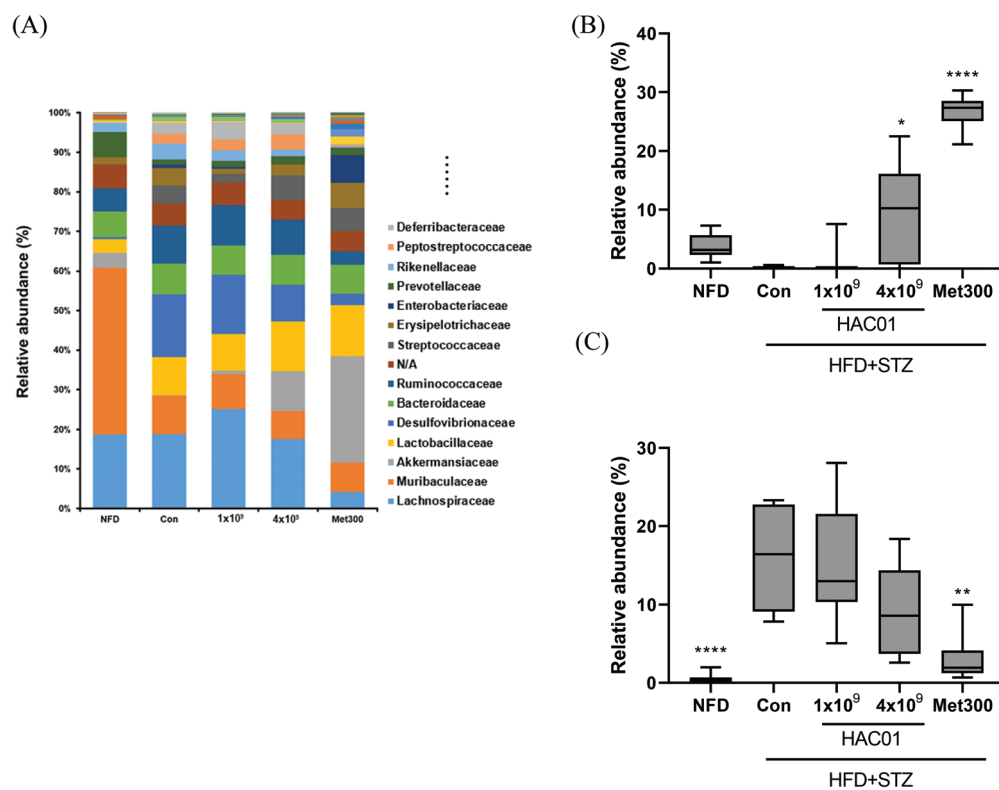


Fig. 6 Changes in the faecal bacterial community of *L. plantarum* HAC01 in HFD + STZ-induced diabetic mice. (A) Average relative abundance of the family in each group. (B) Relative abundance of the family, Akkermansiaceae, in each group. (C) Relative abundance of the family, Desulfovibrionaceae, in each group. Normal fat diet; HFD + STZ_Con: High-fat diet + streptozotocin (STZ); HFD + STZ_1 \times 10⁹–4 \times 10⁹ HAC01: HFD + STZ + 1 \times 10⁹–4 \times 10⁹ CFU day⁻¹ *L. plantarum* HAC01; Met300: Metformin 300 mg kg⁻¹.

from those of the other groups (Fig. 7). Mirroring the α -diversity differences, a difference was observed in the clustering of different dose-treated groups compared to that in the control and metformin-treated groups. Further, the group

administered 4 \times 10⁹ CFU of *L. plantarum* HAC01 showed relatively similar changes to the Met300-treated group compared to the 1 \times 10⁹ CFU of *L. plantarum* HAC01-treated group (Fig. 7).

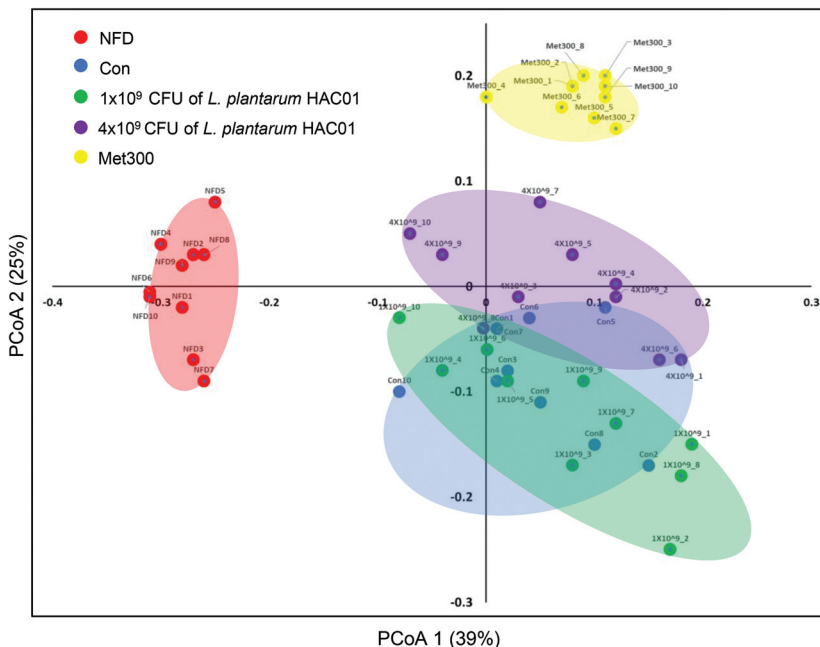


Fig. 7 Principal coordinate analysis (PCoA) plots of the fecal bacterial communities of *L. plantarum* HAC01 in HFD + STZ-induced diabetic mice. Plots generated according to weighted UniFrac distance metrics are presented. Each dot represents one mouse ($n = 10$ per group).

3.7. Effects of *L. plantarum* HAC01 on serum SCFAs levels

SCFAs have been reported to exert beneficial effects on human health. As shown in Fig. 8, serum levels of SCFAs (butyric acid, propionic acid, and acetic acid) were decreased in the HFD + STZ_Con group compared to those in the NFD group. Further, butyric acid levels were significantly increased in the feces collected from the groups administered 4×10^9 CFU of *L. plantarum* HAC01 and Met300. However, there was no significant difference in the levels of propionic acid and acetic acid. Such findings suggest that *L. plantarum* HAC01 led to an increase in butyric acid, which could have a beneficial effect in the HFD + STZ-induced diabetic model.

4. Discussion

In the present study, we sought to determine whether *L. plantarum* HAC01 could improve T2DM. Furthermore, we opted to determine its underlying mechanism of action in HFD + STZ-induced diabetic mice. Herein, *L. plantarum* HAC01 lowered blood glucose and HbA1c levels, and ameliorated HOMA-IR, an indicator used to diagnose insulin resistance, in HFD + STZ-induced diabetic mice. Moreover, *L. plantarum* HAC01 inhibited glucose elevation with reduced AUC in OGTT, implying that it can improve glucose intolerance. Based on these findings, *L. plantarum* HAC01 could improve hyperglycemia.

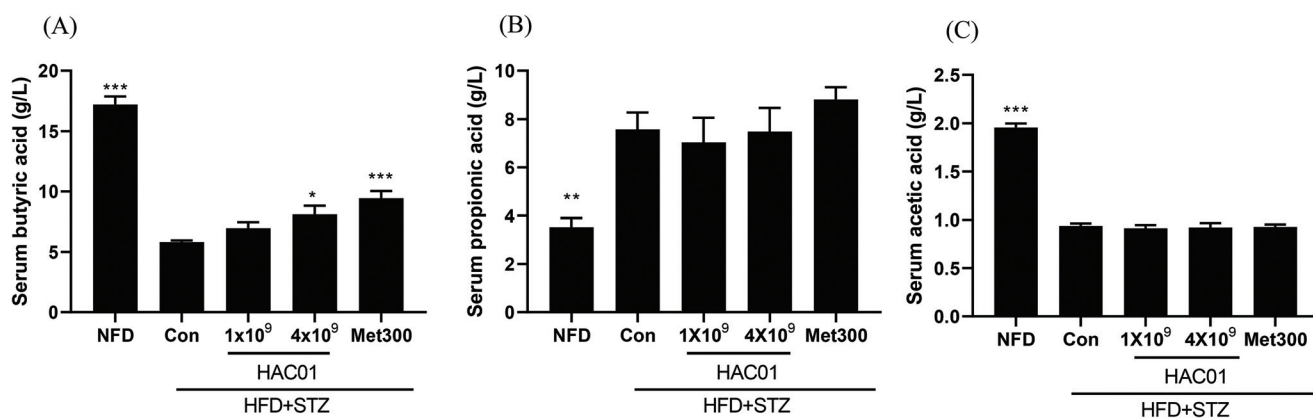


Fig. 8 Effects of *L. plantarum* HAC01 on serum SCFAs levels. The levels of (A) Butyric acid, (B) Propionic acid, and (C) Acetic acid. NFD: Normal fat diet; HFD + STZ_Con: High-fat diet + streptozotocin; HFD + STZ_1 $\times 10^9$ – 4×10^9 HAC01: HFD + STZ + 1×10^9 – 4×10^9 CFU day $^{-1}$ *L. plantarum* HAC01; Met300: Metformin 300 mg kg $^{-1}$. Data are expressed as mean \pm SEM ($n = 10$). * $p < 0.05$ vs. the HFD + STZ_Con group. ** $p < 0.01$ vs. the HFD + STZ_Con group. *** $p < 0.001$ vs. the HFD + STZ_Con group.

mia, insulin resistance, and T2DM and could also prevent or delay the onset of T2DM by ameliorating insulin resistance.

The increase in endogenous glucose production *via* gluconeogenesis is considered to play a primary role in higher fasting blood glucose levels in T2DM. The rate-controlling enzymes of gluconeogenesis, PEPCK and G6Pase, are involved in endogenous glucose production and mainly act *via* the PI3K/Akt and AMPK pathways. Moreover, because the ability to secrete insulin is dependent on the function and mass of islet β cells, the impairment of islet β cells contributes to diabetes.²⁶ In the present study, *L. plantarum* HAC01 was found to exhibit a protective and restorative effect on islet β cells and tended to increase serum insulin levels. In addition, *L. plantarum* HAC01 was found to increase Akt and AMPK phosphorylation and decrease PEPCK and G6Pase mRNA expression levels in the liver. Such findings indicate that *L. plantarum* HAC01 contributes to the improvement of hyperglycemia and T2DM, which may be due to the inhibition of gluconeogenesis and glucose production through the activation of the Akt and AMPK pathways.

As dysbiosis of the gut microbiome may reshape intestinal barrier functions and host metabolic and signaling pathways, which are directly or indirectly related to T2DM, dysbiosis of the gut microbiome is considered to be a factor involved in the pathogenesis of T2DM.⁵ Supplementation with *L. plantarum* HAC01 changed the intestinal microbiome; However, the shift in the microbial community following probiotic administration exhibited differently by treated dose. In the microbiota analysis, treatment with 1×10^9 *L. plantarum* HAC01 resulted in a community similar to that of the control group. However, treatment with 4×10^9 CFU of *L. plantarum* HAC01 increased the population of the family, Akkermansiaceae (phylum Verrucomicrobia), and decreased the population of the family, Dusulfovibrionaceae (phylum Proteobacteria), aligning with the findings obtained after metformin treatment. Several studies have demonstrated that the significant change in microbiota composition following metformin treatment, which is caused by intestinal permeability, is represented by an increase in the population of *Akkermansia muciniphila*.²⁷⁻²⁹ *Akkermansia muciniphila* is a mucin-degrading bacterium of the phylum, Verrucomicrobia, which predominantly resides in the mucus layer of the colon; in this layer, it metabolizes unabsorbable carbohydrates and mucin in SCFAs, which is then employed as fuel by goblet cells. Stimulated goblet cells further produce mucin, leading to thickening of the mucus layer, a decrease in epithelial permeability, and an increase in insulin sensitivity.^{30,31} Regarding to gut barrier function, *L. plantarum* HAC01 tended to increase the expression levels of genes associated with gut barrier function (Fig. S4†). Although more studies are needed to identify active substances from *L. plantarum* HAC01, it is rather intriguing that *L. plantarum* HAC01 increased the population of the family Akkermansiaceae. *L. plantarum* HAC01 could thus be administered to ameliorate gut microbiome dysbiosis and is thus a potential probiotic against T2DM.

Moreover, there has been increasing evidence of the beneficial effect of SCFAs on glucose, lipid homeostasis, obesity, and insulin sensitivity in humans and animals.³²⁻³⁷ The SCFA, butyric acid, might play an important role in blood glucose regulation. Butyric acids promote the proliferation, differentiation, and function of β -cells and are also involved in β -cell mass and glucose-mediated insulin secretion through SCFA receptor-mediated signaling.^{38,39} Butyric acids also enhance glycogen synthesis and increase hepatic glycogen storage in the liver;⁴⁰⁻⁴³ however, by modulating AMPK activity and facilitating insulin signaling, these acids reduce gluconeogenesis through the inhibition of HDACs-mediated overexpression of PEPCK and G6Pase.^{40,42} Owing to the above effects, butyric acid is considered to be an attractive gut product for the treatment of T2DM. In the present study, *L. plantarum* HAC01 significantly increased serum butyric acid levels, similar to metformin. As mentioned above, *L. plantarum* HAC01 reduced the expression levels of genes involved in gluconeogenesis through activation of the AMPK and Akt pathways in the liver. Such findings suggest that *L. plantarum* HAC01 can decrease endogenous glucose production in the liver, which may be accompanied by butyric acid – AMPK and PI3K/Akt pathways.

Because gut-derived products from the intestine are transported to the liver through the portal vein and bile acids are released from the liver to the intestine,⁴⁴ emerging evidence often refers to the relationship between the gut microbiome and the liver. The gut microbiome may thus contribute to improvements in liver disease owing to its composition, intestinal permeability, as well as products and metabolites that can translocate to the liver through the portal vein. As discussed above, *L. plantarum* HAC01 restored the dysbiosis of the gut microbiome, resulting in increased serum butyric acid levels and improved hepatic insulin resistance with increased β cell mass. Based on previous reports and our findings, *L. plantarum* HAC01 may regulate the gut microbiota-SCFAs (butyric acids)-liver axis, thereby ameliorating T2DM.

5. Conclusion

In the present study, *L. plantarum* HAC01 was found to decrease blood glucose levels, improve glucose intolerance, decrease hepatic gluconeogenesis by activating the AMPK and Akt pathways in the liver, restore the composition of gut microbiota, and increase the levels of butyric acid. These findings imply that *L. plantarum* HAC01 could improve hyperglycemia and T2DM by regulating the gut microbiota-liver axis, ultimately supporting its beneficial effect for T2DM treatment.

Author contributions

Y-S L: Designed and performed the experiments, analyzed the data, and wrote the manuscript. D L: Performed the experiments. S-H K and G-S P: Analyzed the fecal microbiota and wrote the manuscript. Y-K L and J P: Analyzed SCFA. J-H K:



Supervised the manuscript. All coauthors contributed to the manuscript and have approved the final manuscript.

Conflicts of interest

The authors report no conflict of interest.

Acknowledgements

This work was funded by the National Research Foundation of Korea (NRF) (Grant number 2016M3A9A592316023).

References

- 1 K. Ogurtsova, J. da Rocha Fernandes, Y. Huang, U. Linnenkamp, L. Guariguata, N. H. Cho, D. Cavan, J. Shaw and L. Makaroff, IDF Diabetes Atlas: Global estimates for the prevalence of diabetes for 2015 and 2040, *Diabetes Res. Clin. Pract.*, 2017, **128**, 40–50.
- 2 D. A. Barrière, C. Noll, G. Roussy, F. Lizotte, A. Kessai, K. Kirby, K. Belleville, N. Beaudet, J.-M. Longpré and A. C. Carpentier, Combination of high-fat/high-fructose diet and low-dose streptozotocin to model long-term type-2 diabetes complications, *Sci. Rep.*, 2018, **8**, 1–17.
- 3 R. Hu, F. Zeng, L. Wu, X. Wan, Y. Chen, J. Zhang and B. Liu, Fermented carrot juice attenuates type 2 diabetes by mediating gut microbiota in rats, *Food Funct.*, 2019, **10**, 2935–2946.
- 4 M. C. Petersen, D. F. Vatner and G. I. Shulman, Regulation of hepatic glucose metabolism in health and disease, *Nat. Rev. Endocrinol.*, 2017, **13**, 572–587.
- 5 S. Sharma and P. Tripathi, Gut microbiome and type 2 diabetes: where we are and where to go?, *J. Nutr. Biochem.*, 2019, **63**, 101–108.
- 6 M. Diamant, E. Blaak and W. De Vos, Do nutrient–gut–microbiota interactions play a role in human obesity, insulin resistance and type 2 diabetes?, *Obes. Rev.*, 2011, **12**, 272–281.
- 7 A. Everard and P. D. Cani, Diabetes, obesity and gut microbiota, *Best Pract. Res., Clin. Gastroenterol.*, 2013, **27**, 73–83.
- 8 X. Li, K. Watanabe and I. Kimura, Gut microbiota dysbiosis drives and implies novel therapeutic strategies for diabetes mellitus and related metabolic diseases, *Front. Immunol.*, 2017, **8**, 1882.
- 9 A. Puddu, R. Sanguineti, F. Montecucco and G. L. Viviani, Evidence for the gut microbiota short-chain fatty acids as key pathophysiological molecules improving diabetes, *Mediators Inflammation*, 2014, **2014**, 162021.
- 10 E. E. Canfora, R. C. Meex, K. Venema and E. E. Blaak, Gut microbial metabolites in obesity, NAFLD and T2DM, *Nat. Rev. Endocrinol.*, 2019, **15**, 261–273.
- 11 H. Panwar, H. M. Rashmi, V. K. Batish and S. Grover, Probiotics as potential biotherapeutics in the management of type 2 diabetes—prospects and perspectives, *Diabetes Metab. Res. Rev.*, 2013, **29**, 103–112.
- 12 S. Singh, R. Sharma, S. Malhotra, R. Pothuraju and U. Shandilya, *Lactobacillus rhamnosus* NCDC17 ameliorates type-2 diabetes by improving gut function, oxidative stress and inflammation in high-fat-diet fed and streptozotocin-treated rats, *Benefic. Microbes*, 2017, **8**, 243–255.
- 13 C. Hill, F. Guarner, G. Reid, G. R. Gibson, D. J. Merenstein, B. Pot, L. Morelli, R. B. Canani, H. J. Flint and S. Salminen, Expert consensus document: The International Scientific Association for Probiotics and Prebiotics consensus statement on the scope and appropriate use of the term probiotic, *Nat. Rev. Gastroenterol. Hepatol.*, 2014, **11**, 506.
- 14 A. S. Andreasen, N. Larsen, T. Pedersen-Skovsgaard, R. M. Berg, K. Møller, K. D. Svendsen, M. Jakobsen and B. K. Pedersen, Effects of *Lactobacillus acidophilus* NCFM on insulin sensitivity and the systemic inflammatory response in human subjects, *Br. J. Nutr.*, 2010, **104**, 1831–1838.
- 15 H. S. Ejtahed, J. Mohtadi-Nia, A. Homayouni-Rad, M. Niafar, M. Asghari-Jafarabadi and V. Mofid, Probiotic yogurt improves antioxidant status in type 2 diabetic patients, *Nutrition*, 2012, **28**, 539–543.
- 16 F.-C. Hsieh, C.-L. Lee, C.-Y. Chai, W.-T. Chen, Y.-C. Lu and C.-S. Wu, Oral administration of *Lactobacillus reuteri* GMNL-263 improves insulin resistance and ameliorates hepatic steatosis in high fructose-fed rats, *Nutr. Metab.*, 2013, **10**, 1–14.
- 17 X. Li, E. Wang, B. Yin, D. Fang, P. Chen, G. Wang, J. Zhao, H. Zhang and W. Chen, Effects of *Lactobacillus casei* CCFM419 on insulin resistance and gut microbiota in type 2 diabetic mice, *Benefic. Microbes*, 2017, **8**, 421–432.
- 18 C. Mantegazza, P. Molinari, E. D'Auria, M. Sonnino, L. Morelli and G. V. Zuccotti, Probiotics and antibiotic-associated diarrhea in children: A review and new evidence on *Lactobacillus rhamnosus* GG during and after antibiotic treatment, *Pharmacol. Res.*, 2018, **128**, 63–72.
- 19 Z. Zeng, Q. Yuan, R. Yu, J. Zhang, H. Ma and S. Chen, Ameliorative effects of probiotic *lactobacillus paracasei* NL41 on insulin sensitivity, oxidative stress, and beta-cell function in a type 2 diabetes mellitus rat model, *Mol. Nutr. Food Res.*, 2019, **63**, 1900457.
- 20 S. Park, Y. Ji, H. Park, K. Lee, H. Park, B. R. Beck, H. Shin and W. H. Holzapfel, Evaluation of functional properties of lactobacilli isolated from Korean white kimchi, *Food Control*, 2016, **69**, 5–12.
- 21 S. Park, Y. Ji, H.-Y. Jung, H. Park, J. Kang, S.-H. Choi, H. Shin, C.-K. Hyun, K.-T. Kim and W. H. Holzapfel, *Lactobacillus plantarum* HAC01 regulates gut microbiota and adipose tissue accumulation in a diet-induced obesity murine model, *Appl. Microbiol. Biotechnol.*, 2017, **101**, 1605–1614.
- 22 J. G. Caporaso, C. L. Lauber, W. A. Walters, D. Berg-Lyons, J. Huntley, N. Fierer, S. M. Owens, J. Betley, L. Fraser and M. Bauer, Ultra-high-throughput microbial community

analysis on the Illumina HiSeq and MiSeq platforms, *ISME J.*, 2012, **6**, 1621–1624.

23 J. G. Caporaso, J. Kuczynski, J. Stombaugh, K. Bittinger, F. D. Bushman, E. K. Costello, N. Fierer, A. G. Pena, J. K. Goodrich and J. I. Gordon, QIIME allows analysis of high-throughput community sequencing data, *Nat. Methods*, 2010, **7**, 335–336.

24 P. Yilmaz, L. W. Parfrey, P. Yarza, J. Gerken, E. Pruesse, C. Quast, T. Schweer, J. Peplies, W. Ludwig and F. O. Glöckner, The SILVA and “all-species living tree project (LTP)” taxonomic frameworks, *Nucleic Acids Res.*, 2014, **42**, D643–D648.

25 C. Lozupone, M. E. Lladser, D. Knights, J. Stombaugh and R. Knight, UniFrac: an effective distance metric for microbial community comparison, *ISME J.*, 2011, **5**, 169–172.

26 M. Stumvoll, B. J. Goldstein and T. W. Van Haeften, Type 2 diabetes: principles of pathogenesis and therapy, *Lancet*, 2005, **365**, 1333–1346.

27 S. Y. Geerlings, I. Kostopoulos, W. M. De Vos and C. Belzer, Akkermansia muciniphila in the human gastrointestinal tract: when, where, and how?, *Microorganisms*, 2018, **6**, 75.

28 Y. Naito, K. Uchiyama and T. Takagi, A next-generation beneficial microbe: Akkermansia muciniphila, *J. Clin. Biochem. Nutr.*, 2018, **63**, 33–35.

29 A. Iulia-Suceveanu, S. I. Micu, C. Voinea, M. E. Manea, D. Catrinoiu, L. Mazilu, A. P. Stoian, I. Parepa, R. A. Stoica and A.-P. Suceveanu, Metformin and its benefits in improving gut microbiota disturbance in diabetes patients, *IntechOpen*, 2019, 88749.

30 N.-R. Shin, J.-C. Lee, H.-Y. Lee, M.-S. Kim, T. W. Whon, M.-S. Lee and J.-W. Bae, An increase in the Akkermansia spp. population induced by metformin treatment improves glucose homeostasis in diet-induced obese mice, *Gut*, 2014, **63**, 727–735.

31 J. De La Cuesta-Zuluaga, N. T. Mueller, V. Corrales-Agudelo, E. P. Velásquez-Mejía, J. A. Carmona, J. M. Abad and J. S. Escobar, Metformin is associated with higher relative abundance of mucin-degrading Akkermansia muciniphila and several short-chain fatty acid-producing microbiota in the gut, *Diabetes Care*, 2017, **40**, 54–62.

32 K. Bouter, G. Bakker, E. Levin, A. Hartstra, R. Kootte, S. Udayappan, S. Katiraei, L. Bahler, P. Gilijamse and V. Tremaroli, Differential metabolic effects of oral butyrate treatment in lean versus metabolic syndrome subjects, *Clin. Transl. Gastroenterol.*, 2018, **9**, 155.

33 L. Qu, J. Ren, L. Huang, B. Pang, X. Liu, X. Liu, B. Li and Y. Shan, Antidiabetic effects of Lactobacillus casei fermented yogurt through reshaping gut microbiota structure in type 2 diabetic rats, *J. Agric. Food Chem.*, 2018, **66**, 12696–12705.

34 A. Wahlström, S. I. Sayin, H.-U. Marschall and F. Bäckhed, Intestinal crosstalk between bile acids and microbiota and its impact on host metabolism, *Cell Metab.*, 2016, **24**, 41–50.

35 G. Wang, X. Li, J. Zhao, H. Zhang and W. Chen, Lactobacillus casei CCFM419 attenuates type 2 diabetes via a gut microbiota dependent mechanism, *Food Funct.*, 2017, **8**, 3155–3164.

36 F. Yan, N. Li, J. Shi, H. Li, Y. Yue, W. Jiao, N. Wang, Y. Song, G. Huo and B. Li, Lactobacillus acidophilus alleviates type 2 diabetes by regulating hepatic glucose, lipid metabolism and gut microbiota in mice, *Food Funct.*, 2019, **10**, 5804–5815.

37 L. Zhao, F. Zhang, X. Ding, G. Wu, Y. Y. Lam, X. Wang, H. Fu, X. Xue, C. Lu and J. Ma, Gut bacteria selectively promoted by dietary fibers alleviate type 2 diabetes, *Science*, 2018, **359**, 1151–1156.

38 D. P. Christensen, M. Dahllöf, M. Lundh, D. N. Rasmussen, M. D. Nielsen, N. Billestrup, L. G. Grunnet and T. Mandrup-Poulsen, Histone deacetylase (HDAC) inhibition as a novel treatment for diabetes mellitus, *Mol. Med.*, 2011, **17**, 378–390.

39 C. H. Kim, J. Park and M. Kim, Gut microbiota-derived short-chain fatty acids, T cells, and inflammation, *Immune Netw.*, 2014, **14**, 277.

40 S. Khan and G. Jena, The role of butyrate, a histone deacetylase inhibitor in diabetes mellitus: experimental evidence for therapeutic intervention, *Epigenomics*, 2015, **7**, 669–680.

41 S.-M. Jeon, Regulation and function of AMPK in physiology and diseases, *Exp. Mol. Med.*, 2016, **48**, e245–e245.

42 G.-X. Hu, G.-R. Chen, H. Xu, R.-S. Ge and J. Lin, Activation of the AMP activated protein kinase by short-chain fatty acids is the main mechanism underlying the beneficial effect of a high fiber diet on the metabolic syndrome, *Med. Hypotheses*, 2010, **74**, 123–126.

43 Z. Gao, J. Yin, J. Zhang, R. E. Ward, R. J. Martin, M. Lefevre, W. T. Cefalu and J. Ye, Butyrate improves insulin sensitivity and increases energy expenditure in mice, *Diabetes*, 2009, **58**, 1509–1517.

44 A. Albillos, A. De Gottardi and M. Rescigno, The gut-liver axis in liver disease: Pathophysiological basis for therapy, *J. Hepatol.*, 2020, **72**, 558–577.

